EPJ Web of Conferences **99**, 10004 (2015)
DOI: 10.1051/epjconf/20159910004

Study of charm production in the forward cone at energy $E_{Lab} \sim 75$ TeV with a two-storey X-ray emulsion chamber exposed at, mountain altitudes

A.S. Borisov[1,a], A.P. Chubenko[1], V.G. Denisova[1], V.I. Galkin[2], Z.M. Guseva[1], E.A. Kanevskaya[1], M.G. Kogan[1], V.N. Kulikov[4], A.E. Morozov[1], R.A. Mukhamedshin[3], V.S. Puchkov[1], S.I. Nazarov[2], S.E. Pyatovsky[1], G.P. Shoziyoev[1], M.D. Smirnova[1], and A.V. Vargasov[1]

[1] P.N.Lebedev Physical Institute of the Russian Academy of Sciences, Moscow, Russia
[2] Institute of Nuclear Physics, M.V. Lomonosov Moscow State University, Moscow, Russia
[3] Institute for Nuclear Research of the Russian Academy of Sciences, Moscow, Russia
[4] TSNIIMash, Moscow region, Korolyev, Russia

Abstract. The origin of the cosmic ray hadron excess observed in a deep uniform lead X-ray emulsion chamber (XREC) at depths larger than 70 radiation lengths is analyzed. We present preliminary experimental data on the absorption of cosmic ray hadrons in the two-storey XREC with a large air gap exposed at the Tien Shan mountains. The design of the chamber was especially invented to prove the hypothesis on a substantial increase of the charm particle production cross section with energy at $E_{Lab} \sim 75$ TeV as the main source of the darkness spot excess observed on X-ray films. Experimental data obtained with both a 2-storey XREC and a deep uniform XREC are compared with simulation results calculated with the FANSY 1.0 model. The comparison reveals a qualitative agreement between experimental and simulated data under the assumption of high values of charm particle production cross section at $E_{Lab} \sim 75$ TeV in the forward kinematic region at $x_{Lab} > 0.1$.

1. Introduction

A slowing down of the absorption of high energy (tens of TeV) hadron cascades was observed at the Tien Shan High-Mountain Research Station (TSS) in extensive air shower (EAS) experiments with the Big Ionization Calorimeter (BIC) of 36 m^2 area (Fig. 1) which contained lead absorber of 850-g/cm^2 thick [1,2]. Correspondingly, the attenuation length $L(E_h)$ of the hadronic component of EAS cores increases with energy, E_h, released by hadronic cores in the calorimeter (Fig. 2). To explain the effect, the hypothesis of the existence of the so-called long-flying cosmic ray component was introduced [2,3].

An abnormally weak absorption of hadrons was also soon observed [4] in the Pamir experiment while exposing deep uniform XRECs lead 110 cm thick (Fig. 3). In the range of $t < 70$ radiation lengths, the absorption curve obeys the conventional exponential law with index $\lambda_{abs}^{(1)} = 200 \pm 5$ g/cm^2. However, at larger depths $t > 70$ r.l., the absorption length of hadrons in lead changes and becomes as high as $\lambda_{abs}^{(1)} = 340 \pm 80$ g/cm^2 (Fig. 4).

It was soon suggested [5,6] that both phenomena, i.e., excess ionization in the hadron calorimeter and hadron excess in the deep uniform XREC, result from high values of the cross section of production of leading charm particles (D mesons and Λ_c^+ hyperons) at energies $E_{Lab} \sim 50$ TeV.

To attain a good fit of the experimental data with simulation calculations, it was necessary to assume that the forward-cone charm production cross section rapidly increases with energy and amounts to $\sigma_{c\bar{c}}^{NN} \simeq 2-4$ mb at $E_h \gtrsim 20$ TeV in the forward kinematic region $x_{Lab} \gtrsim 0.1$. Note, that in the early 1990s, when attainable accelerator energies were only $\sqrt{s} = 20-50$ GeV, the measured values of charm production cross section were as small as tens of μb. This means that the charm production cross section should rapidly (almost linearly) increase with energy that contradicted theoretical approaches available at that time.

To prove this hypothesis, a dedicated experiment was proposed [7] which employs a two-storey XREC with a large air gap between two vertically separated lead blocks of the chamber (Fig. 5).

The main idea of the experiment is to allow charmed particles to decay effectively within a gap of width $H \simeq c\tau\gamma = c\tau \cdot E/m \approx 2.5$ m emitting $e^{\pm}$ particles and γ-rays within leptonic and semileptonic decay modes. Here τ is the life-time of D mesons, γ, E and m are their Lorentz factor, energy and mass respectively. The emitted electromagnetic particles will generate electromagnetic cascades in the lower lead block and will thus manifest themselves as a bump on the absorption curve (Fig. 6) while high energy electromagnetic particles produced by cosmic rays above the chamber will be effectively screened out by the upper lead block. The magnitude of the bump should obviously correlate with the value of charm production cross section. Such experiments have been recently carried out at the TSS and are now going on at the Pamirs.

[a] e-mail: borisov@sci.lebedev.ru

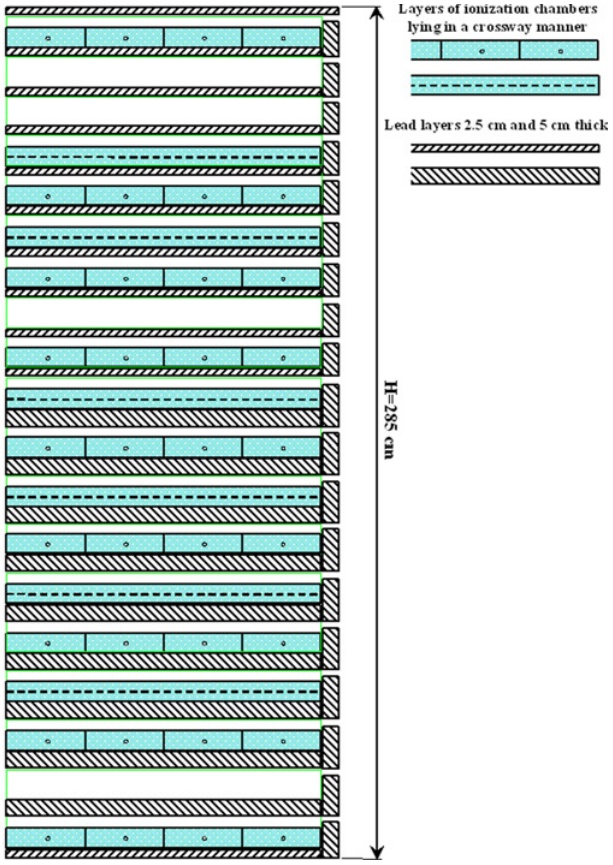

Figure 1. Profile of the Big Ionization Chamber 36 m^2 in area with lead absorber 850-g/cm^2 thick exposed at the Tien Shan Station in 1974.

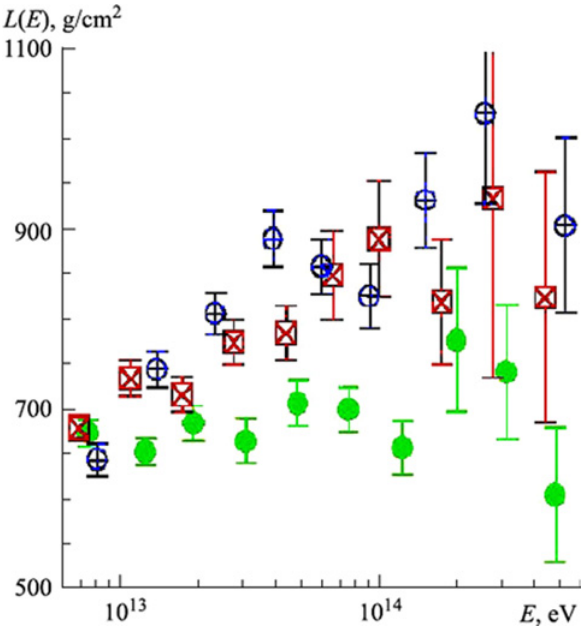

Figure 2. Attenuation length $L(E)$ of hadronic component in EAS cores observed with ionization calorimeter: crossed circles show experimental data. Monte Carlo simulation results are shown with solid circles (zero charm production cross section in accordance with low energy hadronic models, $P(\chi^2) < 10^{-4}$), crossed squares ($(\sigma^{prod}_{h\to c} \approx 0.3 \cdot \sigma^{inel}_{hPb})$, $P(\chi^2) = 0.16$).

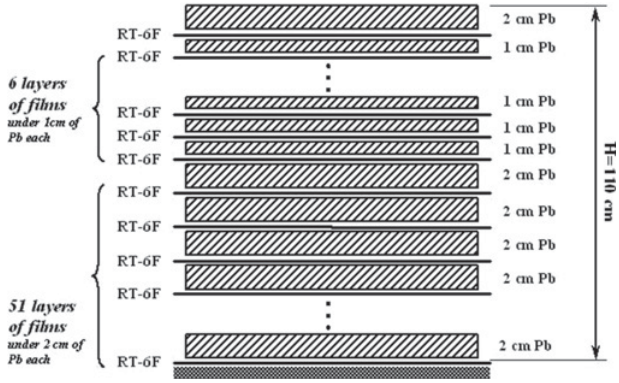

Figure 3. Profile of the deep uniform lead XREC 110-cm thick exposed in the Pamir experiment.

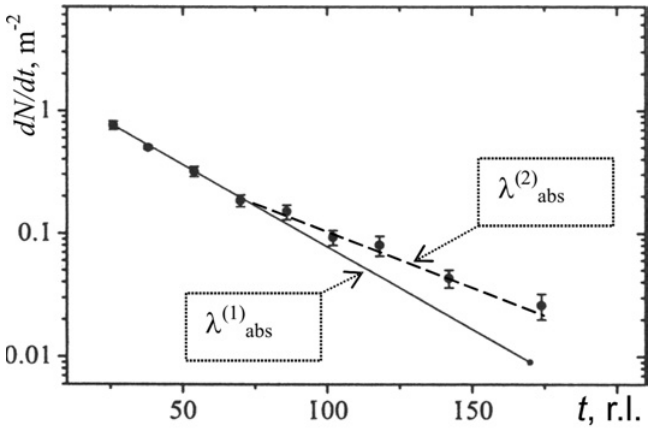

Figure 4. Distribution of hadron-cascade origin points in deep uniform lead XREC 110-cm thick in the framework of the Pamir experiment ($E_h^{(\gamma)} \geq 6.3$ TeV).

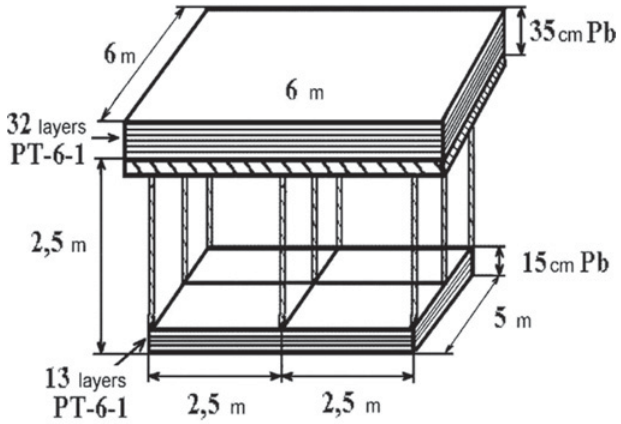

Figure 5. Lay-out of 2-storey XREC with 2.5-m air-gap (a project by L.G. Sveshnikova *et al.*).

This work presents an analysis of experimental data on the absorption of cosmic ray hadrons obtained during a one year exposure (2007 – 2008) of the two-storey XREC with large air gap at the TSS. The experimental data are compared with simulated ones assuming various values of charm production cross section. The same comparison is performed for experimental data of the Pamir experiment with deep (110-cm thick) uniform lead XREC.

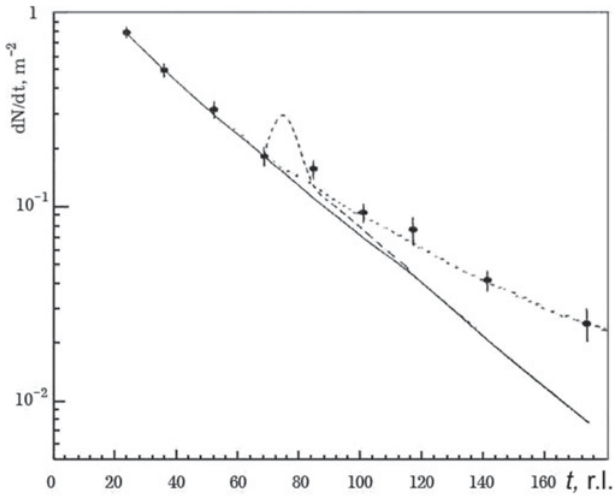

Figure 6. Distribution of cascade origin points in deep uniform lead chamber and in two-storied XREC with 2.5-m air-gap (illustration): solid line stands for absorption according to the conventional exponential law with index $\lambda^{(1)}_{abs} = 200 \pm 5$ g/cm^2; dotted line shows Monte Carlo simulation results for deep uniform XREC accounting for a long-flying component with absorption length $\lambda^{(2)}_{abs} = 340 \pm 80$ g/cm^2.

2. Design and some specific features of the two-storey XREC

To construct a two-storey XREC with a large air gap between two lead blocks we take advantage of specific features of a two storey laboratory building at the Tien Shan Station located at an altitude of 3300 m above sea level (700 g/cm^2). This building has a "window" in the floor slabs between the storeys. The XREC was assembled at the top of the ionization calorimeter, the height of which limited the width of the air gap to 2.16 m (unfortunately, the ionization calorimeter was not put into operation during the exposure of the two-storey XREC and thus did not provide any additional experimental data).

The final design of the two-storey XREC, exposed at the TSS for one year 2007 – 2008, consisted of the upper and lower blocks with areas of 48 m^2 and 32 m^2 respectively, and 2.16 m air gap between them (Fig. 7). The lead plates of both blocks were interleaved with X-ray films of RT-6F type manufactured in Russia. The X-ray films were used as sensitive elements of the chamber.

The upper block of the chamber consisted of a so-called Γ-block containing three layers of X-ray films under 3.5, 5.0 and 6.5 cm of lead and a conventional Pb-block which were separated by two rows of ionization chambers and a 1.5 cm thick lead absorber between them. The Pb-block has 23 lead layers. The thickness of the first lead layer is 2 cm, while other lead layers are each 1 cm thick. In the central part of the Pb-block, the lead layers are interleaved with X-ray films covering only 12 m^2 of its total area. Thus the total depth of the lead absorber in the upper block is 32 cm. Until now only the 1st, 2nd, 4th, 9th, 10th, 14th, 20th and 2lst layers of X-ray films of the Pb-block have been treated carefully.

The lower block of the two-storey XREC includes thirteen layers of X-ray films. The first layer is placed

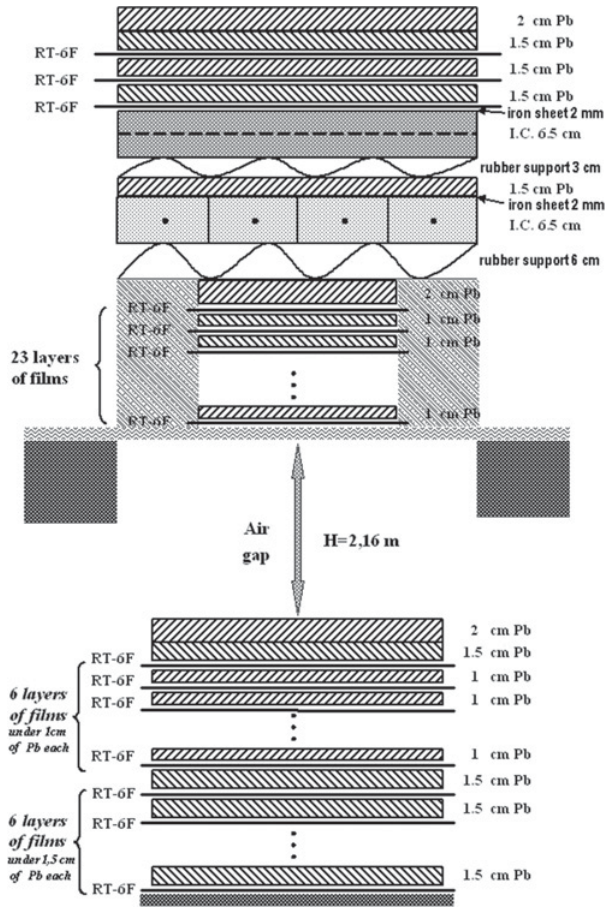

Figure 7. Profile of the two-storey XREC with 2.16-m air gap 48/32 m^2 in area exposed at TSS in 2007–2008.

Figure 8. Photo of the upper block of the two-storey XREC exposed at TSS in 2007–2008.

under 3.5 cm of lead; the next six X-ray film layers are separated by 1 cm of lead, and the last six film layers are separated by 1.5 cm of lead. Until now only the first four and 6th, 7th and 12th X-ray film layers of the lower block have been treated.

Photos of the upper and lower blocks are shown in Figs. 8 and 9, respectively.

The electromagnetic component of cosmic rays incident on the XREC is almost completely absorbed in the Γ-block. Taking into account the additional lead layer 1.5 cm thick and spacing effects due to the presence of

Figure 9. Photo of the lower block of the two-storey XREC exposed at TSS in 2007–2008.

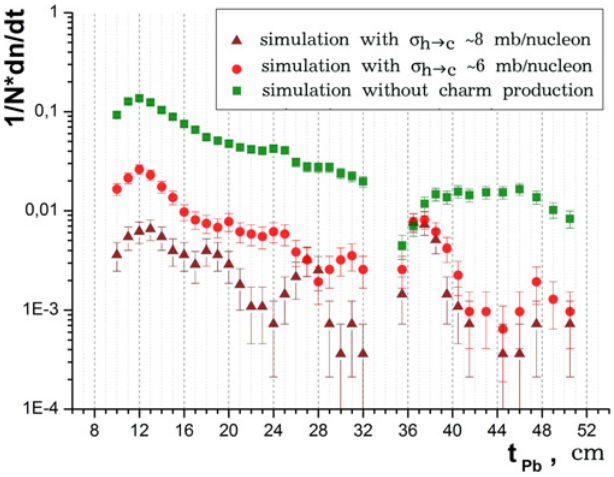

Figure 10. Simulated distributions of darkness spots with optical densities D > D_{min}=0.4 produced by hadron cascades in XREC with air gap as a function of lead depth t (simulation according to ECSim2.0@FANSY code with three options for charm production cross section $\sigma^{fragm}_{h\to charm}$: (1) ∼ 0 (green squares); (2) ∼ 6 mb/nucleon (red circles); (3) ∼ 8 mb/nucleon (brown triangles).

two layers of rubber supporters (3 and 6 cm thick each) as well as two layers of ionization chambers with thin copper casing, darkness spots observed in the 23 X-ray film layers of the Pb-block are only produced by cosmic ray hadrons in their interactions with lead. Thus the hadron-induced showers are the only source of darkness spots observed in the Pb-block. The estimated threshold energy of the recorded hadron-induced cascades is ∼6–8 TeV.

Due to the large 2.16-m air gap between the two blocks of the two-storey XREC the hadron-induced showers originating in the upper block practically vanish in the gap. Only penetrating hadrons and successive hadronic interactions in the lead absorber of the lower block can produce darkness spots on X-ray films placed in the lower block.

Therefore, we should observe a drastic decrease of the darkness spot intensity in the first six centimeters of the lower block if it were not for charm production. Charm particles produced in the upper block effectively decay in the air gap, partially emitting electromagnetic particles which, in their turn, should generate electromagnetic showers in the lead absorber of the lower block.

Nowadays the experiment with a two-storey XREC, which has an optimal air gap 2.5-m wide, is going on at the Pamirs at an altitude of 4360 m a.s.l. (595 g/cm^2) where the hadron flux intensity is almost three times higher than the intensity of cosmic ray hadrons at the TSS.

3. Simulation of the experiment and the XREC response

Monte-Carlo simulations of both experiments, i.e., with the two-storey XREC and deep homogeneous lead XREC, were carried out assuming that the incident cosmic ray hadrons at mountain altitudes are mainly represented by nucleons and pions with energies $E_h \geq 20$ TeV and that these are produced by protons and nuclei of the primary cosmic ray radiation in the thick target (700 g/cm^2) of the atmosphere above the chamber. It was assumed that relative fractions of incident nucleons and pions are 60% and 40% while indices of power energy spectra for nucleons and pions are −3.10 and −3.22, respectively.

Nuclear-electromagnetic cascades produced by incident nucleons and pions in XREC of both types were simulated with the software package ECSim2.0 [8]. The ECSim 2.0 code is based on the GEANT3.21 package and allows to calculate the detector response for XREC of a given design taking into account the exact experimental technique employed in the Pamir experiment including processing and measurement of darkness spots produced by electromagnetic cascades on X-ray films.

To generate nucleon-lead and pion-lead interactions accounting for the production of charm hadrons and their subsequent decay in the air gap with the emission of $e^{\pm}$ and γ-rays, the FANSY1.0 model [9] was used and incorporated in the ECSim 2.0 package. The FANSY1.0 Monte Carlo generator represents a phenomenological hadronic interaction model based on quark-gluon string theoretical approaches and assumes charm particle production with various cross sections. In many features it is close to the QGSGET II model. However, in pp interactions x_F spectra of secondary particles including charmed ones appeared to be too soft as compared to the LHC data.

To make results of the experiment, which are derived from comparing experimental data on the absorption of hadrons in XREC with simulated ones, more robust to experimental errors and fluctuations in the development of nuclear-electro-magnetic cascades taking into account limited experimental statistics, we treated not only reconstructed individual cascades but also separate darkness spots as we observe them at each film layer, i.e., quite independently from layer to layer. This procedure increases the statistics of the experimental data being analyzed and strongly diminishes the experimental ambiguities related to the rather complicated procedure of reconstruction of cascades recorded with multi-layered XRECs.

Simulation results calculated with the ECSim2.0@FANSY 1.0 code for the Tien Shan experiment with the two-storey XREC are presented in Figs. 10 and 11.

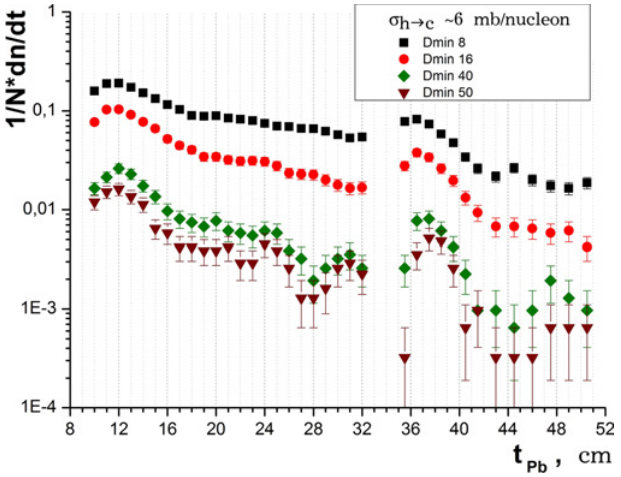

Figure 11. Simulated distributions of darkness spots produced in two-storey XREC with air gap by hadron cascades as a function of lead depth t at different optical density thresholds D_{min} ($D_{min} = 0.08, 0.16, 0.4, 0.5$) for observation of darkness spots (simulation according to ECSim2.0@FANSY 1.0 code).

A lead-absorber-depth dependence of darkness spot number per one X-ray film and per one incident particle is plotted in Fig. 10 for three cases of charm production parameters which determine the following values of charm production cross section $\sigma^{fragm}_{h\to charm}$ in the kinematic forward-cone fragmentation region, i.e., at $x_{Lab} > 0.1$:

1. $\sigma^{fragm}_{h\to charm}$ is close to zero (green squares);
2. $\sigma^{fragm}_{h\to charm}$ is as high as ~ 6 mb/nucleon (red circles).
3. $\sigma^{fragm}_{h\to charm}$ is extremely high, namely, $\sigma^{fragm}_{h\to charm} \sim 8$ mb/nucleon (brown stars).

As follows from Fig. 10, in the case of negligible charm-production cross section $\sigma^{fragm}_{h\to charm} \sim 0$, there is a drastic fall of the spot number in the initial layers of X-ray films in the lower block of the two-storey XREC just after the bottom of the upper block (or after the layer corresponding to 32 cm of lead absorber in the plotted distribution). Then we observe a gradual restoration of distribution points to the same exponential dependence as observed in the upper block of the XREC. Such a behaviour of the darkness spot distribution is explained with a lead-air-lead transition effect taking into account the large width of the air gap and specific features of hadron cascades in lead absorbers which are governed by the large value of the nuclear interaction length ($\lambda^{\pi-Pb}_{int} \approx 10.5$ cm) and a short radiation length in lead ($X_0 \approx 0.56$ cm).

However, if the charm production cross section is as high as $\sigma^{fragm}_{h\to charm} \sim 6-8$ mb/nucleon, we observe (Fig. 10) a bump on the darkness spot distribution at the initial layers of X-ray films in the lower block due to the appearance of electromagnetic showers generated via the decay of charmed particles (such as $D^{\pm}$, D^0, D^* mesons, Λ_c hyperons) in the air gap. The relative amplitude of this bump increases with increasing $\sigma^{fragm}_{h\to charm}$ that makes it possible to measure the value of the charm production cross section at $x_{Lab} \gtrsim 0.1$ in experiments with two-storey XRECs.

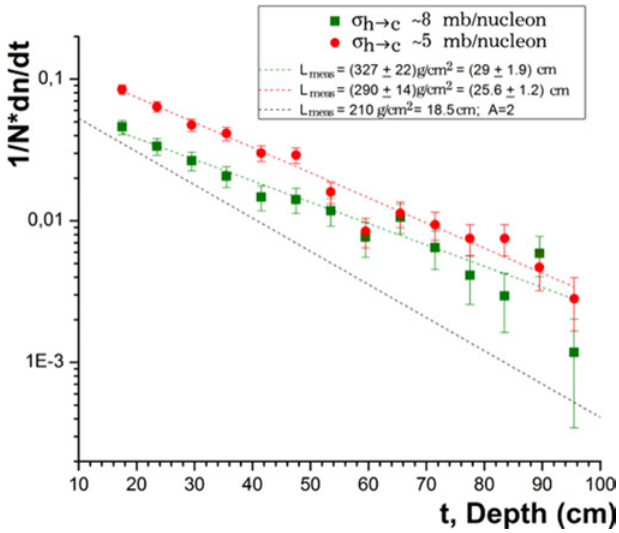

Figure 12. Simulated distributions of hadron cascade origin points produced in homogeneous lead XREC 110-thick at two values of charm production cross section $\sigma^{fragm}_{h\to charm}$, namely, ~ 5 and ~ 8 mb/nucleon, and assuming that the fractionts of nucleons and pions among incident particles are 60% and 40%, respectively (optical density threshold for darkness spot observation is $D_{min} = 0.08$). Lines show $exp((-t/L_{meas}) - A$ dependencies.

This bump appears to be more pronounced with increasing the darkness threshold, D_{min}, for observing the spots (Fig. 11). In addition we observe some shifting of the position of the bump to the depth of the lower block with increasing D_{min}.

We applied the same ECSim2.0@FANSY 1.0 code with high values of charm production cross sections for simulation of the experiment with deep uniform lead XRECs 110-cm thick which were exposed at the Pamirs in the mid 1980s. The exact profile of the deep XREC is shown in Fig. 3.

The simulation results on the distribution of the origin points of hadron cascades calculated for the Pamir experiment with homogeneous absorber 110-cm thick assuming two values of charm production cross section $\sigma^{fragm}_{h\to charm}$, namely, ~ 5 and ~ 8 mb/nucleon, are presented in Fig. 12.

One can see that accounting for charm production leads to an increase of the absorption length of hadron cascades just from the very top of the absorber, so the distribution of the origin points of hadron cascades can be approximated by one exponential law for the whole depth of the absorber. Besides, the slope of the absorption curves strongly depends on the value of the charm production cross section.

4. Comparison of experimental and simulated data

The preliminary experimental distribution of darkness spots observed in the Tien Shan two-storey XREC over lead absorber depth, t, is plotted in Fig. 13. To adequately compare the experimental data with simulation, the experimental distribution was normalized to the simulated

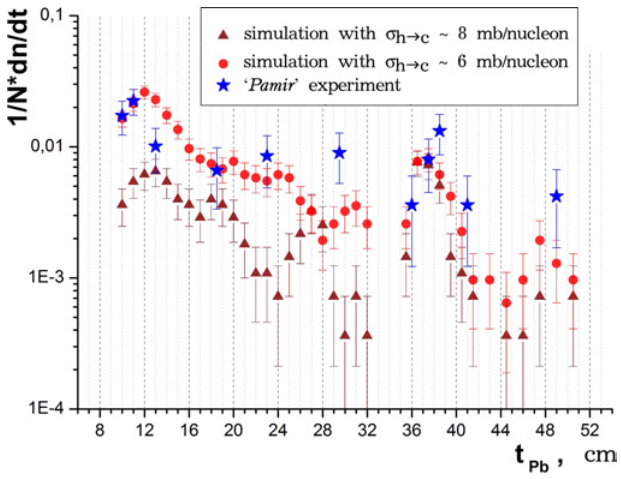

Figure 13. Lead depth dependence of number of darkness spots in the Tien Shan experiment with two-storey XREC: experimental data (number of darkness spots per X-ray film) (blue stars) and simulation results with two different charm production cross sections, i.e., $\sigma^{fragm}_{h\to charm} \sim 6$ mb/nucleon (red circles) and $\sigma^{fragm}_{h\to charm} \sim 8$ mb/nucleon (brown triangles) at optical density threshold for darkness spot observation $D_{min} = 0.40$.

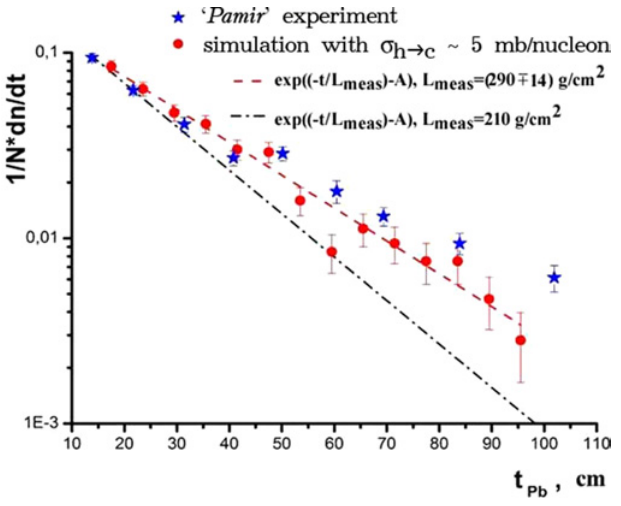

Figure 14. Distributions of hadron cascade origin points produced in homogeneous lead XREC if $\sigma^{fragm}_{h\to charm} \sim 5$ mb/nucleon at $x_{Lab} \gtrsim 0.1$ assuming that the fractions of nucleons and pions among incident particles are 60% and 40%, respectively.

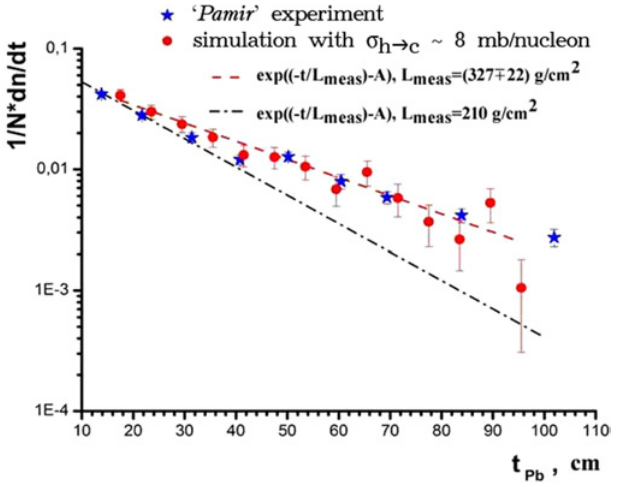

Figure 15. Distribution of hadron cascade origin points produced in homogeneous lead XREC if $\sigma^{fragm}_{h\to charm} \sim 8$ mb/nucleon at $x_{Lab} \gtrsim 0.1$ assuming that the fractions of nucleons and pions among incident particles are 60% and 40%, respectively.

one calculated with $\sigma^{fragm}_{h\to charm} \sim 6$ mb/nucleon at the point corresponding to 10-cm depth of lead in the upper block of the two-storey XREC.

Note that simulated distributions were calculated on the assumption that the observation threshold of the darkness spots on X-ray films $D_{min} = 0.4$, where D is the optical density of the spot. According to our preliminary measurements of spot optical densities, this value of D_{min} is close to the experimental threshold although it should be increased by ~35%.

One can see from Fig. 13 that the simulated distribution corresponding to the case No. 2 fits the experimental data rather well unless you consider some shift in the position of the experimental bump to larger observation depths as compared with simulated distributions.

As shown in Fig. 11 the bump position is sensitive to the optical density threshold D_{min} for observation of the darkness spots, i.e., the bump slightly shifts to the larger lead depths with increasing D_{min}. Thus the observed discrepancy between the experimental data and simulated one can be, partially, explained by higher energy threshold for hadron detection in our experiment.

The same approach for explaining the abnormal behaviour of hadron penetration in lead was applied to the analysis of experimental data obtained with the deep uniform lead XRECs 110 cm thick which were exposed at the Pamirs in the middle of 1980s [4]. The experimental distribution of the cascade origin points for hadrons with $E_h^{(\gamma)} \gtrsim 6.3$ TeV obtained in the Pamir experiment by means of deep uniform XRECs is presented in Fig. 14 and Fig. 15.

The experimental data are compared with simulated ones calculated with the ECSim2.0@FANSY 1.0 code on the assumption of two different values of charm production cross section, namely, $\sigma^{fragm}_{h\to charm} \sim 5$ mb/nucleon (Fig. 14) and $\sigma^{fragm}_{h\to charm} \sim 8$ mb/nucleon at $x_{Lab} > 0.1$ (Fig. 15). As follows from these figures, the data set, simulated with the charm production cross section being as high as $\sigma^{fragm}_{h\to charm} \sim 8$ mb/nucleon, fits the experimental data well enough. However, it does not allow us to distinguish two different components in the hadron flux which obey different exponentials as can be seen in Fig. 4.

5. Discussion

Recently ALICE, LHCb and ATLAS collaborations have measured inclusive transverse momentum spectra of open-charm mesons in proton-proton collisions at $\sqrt{s} = 2.76$ and 7 TeV. These results are very interesting from the theoretical point of view due to the highest collision energy ever achieved in accelerator experiments and due to a unique rapidity acceptance of the detectors.

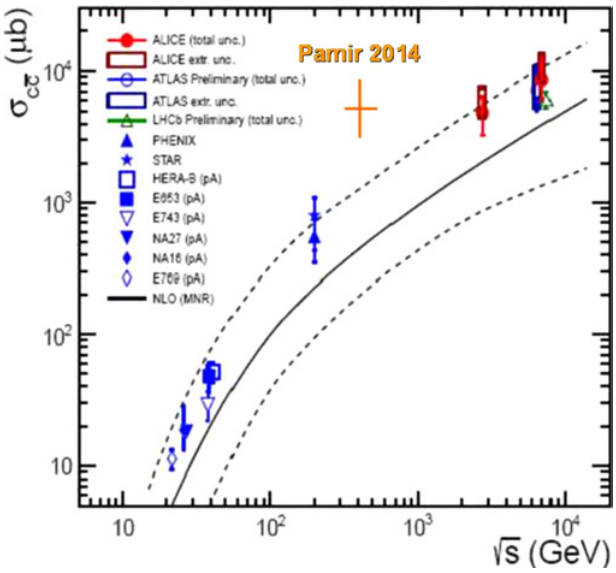

Figure 16. Energy dependence of the total nucleon-nucleon charm production cross section according to experimental data and NLO MNR calculation. The NLO MNR calculation [14] (and its uncertainties) is represented by solid (dashed) lines.

Especially, results from the middle rapidity region $2 < \eta < 4$, obtained by the LHCb, as well as ATLAS data from central pseudorapidity range $\eta < 2.1$ can improve our understanding of pQCD production of heavy quarks (see, e.g., [10–12]).

Unfortunately, particles, produced in the most forward cone of phase space with high values of pseudorapidities η (i.e., in the so-called fragmentation region of a projectile particle), are practically unobservable by colliders due to their specific constructional traits (finite dimension of the acceleration pipe which hinders placing detectors close to the collision axis). On the contrary, cosmic ray experiments with fixed target make it possible to investigate the fragmentation region of projectile particles, i.e., $x_{Lab} \gtrsim 0.1$, where the behaviour of charm production with energy could be different from that observed in the central range. In any case, cosmic ray experiments could give some complementary information to collider data.

The significance of the forward region greatly increases with interaction energy, so that it begins to play a key role at the primary energies under investigation (for instance, at the LHC design energy $E_0 \sim 10^{17}$ eV almost 90% of the collision energy is released in the region with $\eta \geq 5$).

The first evidence of rapid growth of charm hadroproduction cross sections with energy in the mid rapidity range was presented by the STAR/RHIC Collaboration in 2004 [13]. Soon these results were confirmed by the PHENIX Collaboration [14]. A strong energy dependence of the total charm production cross section was revealed: $\sigma_{pp\to c\bar{c}} \sim E^{0.8}$.

Compilation of accelerator data on total charm production cross section, including recent results from LHC experiments, is presented in Fig. 16. The total charm production cross section at $\sqrt{s} = 2.76$ and 7 TeV was evaluated, rather than measured, by extrapolating from the central rapidity range to the full phase space using theoretical models. The experimental data are fitted with simulations performed within the framework of perturbative-QCD (pQCD) approaches accounting for Next-to-Leading Order (NLO) corrections. The NLO pQCD calculation (and its uncertainties) is represented by the solid (dashed) line.

At $\sqrt{s} = 2.76$ and 7 TeV, measurements carried out by the ALICE, ATLAS and LHCb Collaborations are in fair agreement [11] with each other:

$$\sigma^{tot}_{pp\to c\bar{c}}(2.76\ \text{TeV}) = 4.8 \pm 0.8(stat)^{+1.0}_{-1.3}(syst.)\ \text{mb},$$
$$\sigma^{tot}_{pp\to c\bar{c}}(7\ \text{TeV}) = 8.5 \pm 0.5(stat)^{+1.0}_{-2.4}(syst.)\ \text{mb}.$$

To get the values of total charm production cross sections cited above, the measured cross sections were extrapolated to the full phase space by scaling the measured cross section by the ratio of the total cross section over the cross section in the experimentally covered phase space calculated using the NLO pQCD technique.

Taking into account rather large uncertainties of this procedure, one can conclude that cosmic ray experiments provide high energy physicists with complementary information on the charm hadroproduction mechanism.

As follows from comparison of charm production cross sections obtained in accelerator experiments and in cosmic ray experiments (Fig. 16), cosmic ray values seem to be too high. We believe that accounting for high energy incident muons (including so-called prompt muons originating via the decay of charm particles) and an implementation of a harder spectra of secondary particles in the FANSY1.0 model in accordance with recent LHC results will decrease the value of the charm production cross-section. A possible contribution of methodical errors into the experimental data must also be analyzed in detail.

6. Conclusion

The analysis of experimental data obtained in two high altitude experiments with a two-storey XREC and a deep uniform XREC shows that an abnormally weak absorption of hadrons in the thick lead absorber can be explained with a rapid increase of forward-cone charm production cross section $\sigma^{fragm}_{hp\to charm}$ with energy up to such high values as $6 - 8$ mb/nucleon at energies $\langle E^{Lab}_h \rangle \sim 75$ TeV. However, the available experimental statistics do not allow us to exclude other possible hypotheses, for instance, the existence of some additional long-flying cosmic ray component like strangelets which can also contribute to the observed effects.

The work is supported by the Program of fundamental research of the Presidium of the Russian Academy of Sciences “Fundamental properties of Matter and Astrophysics”.

References

[1] V.S. Aseikin, et al.. Izvestiya of AN of USSR, ser. fiz., No 5, p. 998 (1974)
[2] S.I. Nikolsky, E.L. Feinberg, V.P. Pavluchenko, V.I. Yakovlev. Preprint FIAN, N 69 (1975)

[3] I.M. Dremin, V.I. Yakovlev // Topics on Cosmic Rays. 60th Anniversary of C.M.G. Lattes. Campinas, 1984, v. **1**, P. 122
[4] Collaboration of Experiment PAMIR // Izv. AN USSR, Ser. fiz., 1989, v. **53**, No. 2, P. 277
[5] V.I. Yakovlev. Proc. 24th ICRC, Rome (1995) v. **1**, p. 446
[6] I.M. Dremin, D.T. Madigozhin, V.I. Yakovlev // Proc. of the 21st ICRC, Adelaide, 1990, v. **10**, P. 166
[7] L.G. Sveshnikova, O.P. Strogova. Proc. 23rd ICRC, Calgary (1993) v. **4**, p. 33
[8] A.S. Borisov, V.G. Denisova, V.I. Galkin et al. Proc. 30th ICRC, Merida (2007) v. **4**, 593
[9] R.A. Mukhamedshin, 2009 Eur. Phys. J. C **60**, 345
[10] B. Abelev et al. (The ALICE Collaboration), J. High Energy Phys. 01 (2012) 128; The ALICE collaboration. CERN-PH-EP-ALICE-2012-069 October 15, 2012; The ALICE Collaboration. arXiv: 1203.2160v4 [nucl-ex] 12 Oct. 2012; arXiv: 1205.4007v2 [hep-ex] 6 Aug. 2012
[11] The LHCb Collaboration, LHCb-CONF-2010-013
[12] The ATLAS Collaboration, ATLAS-CONF-2011-017
[13] A. Tai, J. Phys. G 30 (2004) S809. The STAR collaboration. arXiv: 1204.4244v3 [nucl-ex] 14 Oct. 2012
[14] S. Kelly, J. Phys. G **30** (2004) S1189